



University of HUDDERSFIELD

University of Huddersfield Repository

Beverley, Katharine J., Clint, John H. and Fletcher, Paul D. I.

Evaporation rates of pure liquids measured using a gravimetric technique

Original Citation

Beverley, Katharine J., Clint, John H. and Fletcher, Paul D. I. (1999) Evaporation rates of pure liquids measured using a gravimetric technique. *Physical Chemistry Chemical Physics*, 1 (1). pp. 149-153. ISSN 1463-9076

This version is available at <http://eprints.hud.ac.uk/id/eprint/16334/>

The University Repository is a digital collection of the research output of the University, available on Open Access. Copyright and Moral Rights for the items on this site are retained by the individual author and/or other copyright owners. Users may access full items free of charge; copies of full text items generally can be reproduced, displayed or performed and given to third parties in any format or medium for personal research or study, educational or not-for-profit purposes without prior permission or charge, provided:

- The authors, title and full bibliographic details is credited in any copy;
- A hyperlink and/or URL is included for the original metadata page; and
- The content is not changed in any way.

For more information, including our policy and submission procedure, please contact the Repository Team at: E.mailbox@hud.ac.uk.

<http://eprints.hud.ac.uk/>

Evaporation rates of pure liquids measured using a gravimetric technique

K. J. Beverley, J. H. Clint and P. D. I. Fletcher*

Surfactant Science Group, Department of Chemistry, University of Hull, Hull, UK HU6 7RX.
E-mail: P.D.Fletcher@chem.hull.ac.uk

Received 9th July 1998, Accepted 13th October 1998

We describe a gravimetric method for the determination of evaporation rates. The liquid sample is held in a partially filled, cylindrical open-topped tube within a vertically flowing gas stream. A simple model appropriate to this geometry is found to account for the variation of rate with liquid height within the sample tube and gas flow rate. Evaporation rates for a range of pure liquids with vapour pressures ranging from 0.1 to 500 Torr were determined and showed reasonable agreement with theoretical values estimated using literature values of the vapour pressures and vapour diffusion coefficients in air.

Evaporation rates are of interest from a number of viewpoints including assessment of hazards arising from the spillage of volatile liquids, release of volatile active components from commercial products and the retardation and control of evaporation by adsorbed monolayers or entrapment of the liquid within a colloidal microstructure. Two main classes of methods for the measurement of evaporation rate have been described in the literature. The first involves the measurement of weight gain of a vapour adsorbent placed above the liquid surface.^{1,2} This method allows relative rates across a quiescent gas space to be determined but does not yield absolute rates which can be related to the physical properties of the evaporating species. The second class involves measurement of the rate of liquid loss into a gas stream flowing horizontally across the liquid surface.^{3,4} In this geometry, the evaporation rate depends in a highly complex manner on the gas flow pattern in addition to the physical properties of the liquid species. In this paper, we describe a simple apparatus for the determination of evaporation rate of a liquid held in a partially filled container within a gas stream flowing in a vertical direction. As will be shown, the evaporation rates measured under these conditions are amenable to a quantitative analysis.

Experimental

Water was purified by reverse osmosis and passed through a Milli-Q reagent water system. The organic liquids n-pentane (Aldrich, 98%), n-hexane (Aldrich, 98%), n-heptane (Rathburn, 98%), n-octane (Lancaster, 99%), n-decane (Avocado, 99%), benzene (Fisons, 99.8%), cyclohexane (RectaPur, 99%) and absolute ethanol (Fisons) were columned twice over alumina to remove polar impurities.

The apparatus for measurement of the evaporation rates is shown in Fig. 1. The liquid sample is contained in a cylindrical glass sample tube (inner diameter 17.8 mm, outer diameter 21 mm) suspended from a Precisa 125A balance. The gas (dry nitrogen) is passed through a column of activated charcoal (Puritube supplied by Phase Sep.) to remove any impurities and a flow meter to record the gas volume flow rate, F ($\text{cm}^3 \text{min}^{-1}$). The purified nitrogen stream flows through a thermostating coil and enters the measurement vessel through an annular opening of approximately 1 mm gap. The gas then flows vertically upwards around the sample tube and emerges from the top of the vessel. In the region of the sample

tube mouth, the vessel diameter is 40 mm. The vessel containing the suspended sample tube is contained within a stirred, thermostatted outer vessel. The evaporation rate is determined from the sample mass loss ($\pm 0.0001 \text{ g}$) recorded on the Precisa balance. The data are logged automatically into an EXCEL spreadsheet using a PC equipped with TAL Technologies WinWedge software which allows data transfer from the RS232 interface of the balance.

A typical plot of sample mass loss *versus* time is shown in Fig. 2. For most of the systems studied here, the change in liquid height with time is negligible and the mass loss plots are accurately linear over the initial time interval. The (initial) evaporation rate is obtained as the slope of the best-fit straight line to the initial time data. The experimental uncertainty in the evaporation rate depends on the accuracy of control of the sample vapour pressure and the gas flow rate. The control of the sample vapour pressure is achieved by temperature control. As will be seen later, the measured rate is proportional to the vapour pressure of the sample and, depending on conditions, either proportional to the gas flow rate or independent of the flow rate. The uncertainty in the

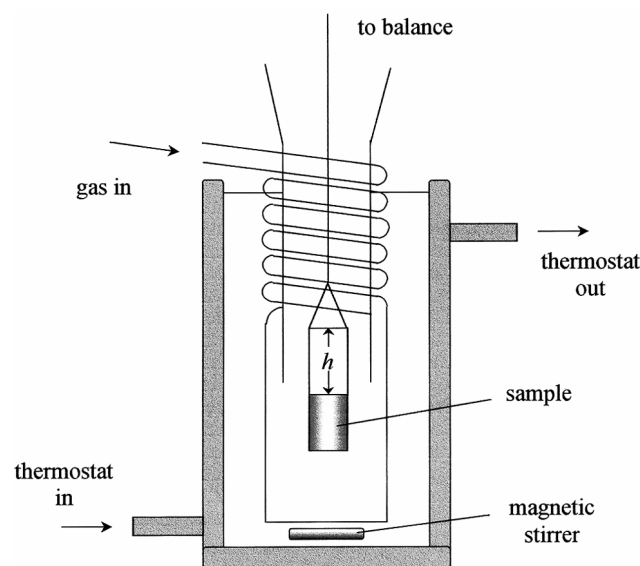


Fig. 1 Schematic diagram of the evaporation rate apparatus.

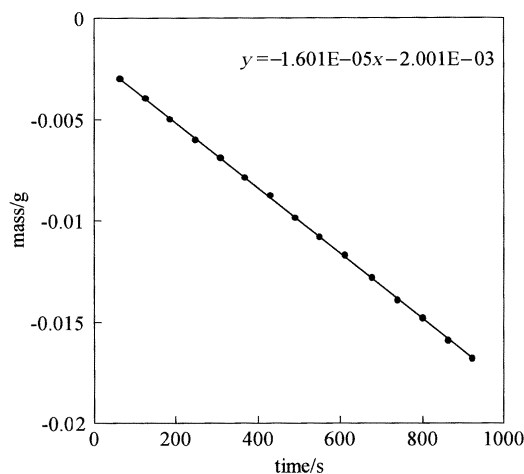


Fig. 2 A typical plot of sample mass versus time. The solid line shows the best fit straight line used to obtain the initial evaporation rate.

sample temperature is $\pm 0.1^\circ\text{C}$ which translates to an uncertainty in the vapour pressure of approximately 1% for the liquid samples used in this study. The uncertainty in the gas flow rate is typically 3% for the flow rates and flow meter used in this work. Hence, the uncertainty in the measured evaporation rates are expected to vary from about 4% (when the rate is proportional to gas flow rate) to 1% (when the rate is independent of flow rate). In practice, repeated measurements show the reproducibility in initial rate is typically 2–5%.

Results and discussion

We first consider the rate of loss of vapour from a pure liquid surface for which there are no external resistances or barriers to the evaporation.⁵ For a liquid in equilibrium with its vapour, the number of molecules striking and condensing with the surface from the vapour must be equal to the number evaporating. The number of molecules striking unit area of surface per unit time is readily calculated using kinetic theory of gases. It is assumed that a fraction α of these molecules condense with the surface. Thus, the maximum possible evaporation flux J_{max} ($\text{mol s}^{-1} \text{m}^{-2}$) into a perfect vacuum is given by the following expression in which α is assumed to be unity.

$$J_{\text{max}} = \frac{P}{\sqrt{2\pi MRT}} \quad (1)$$

In eqn. (1), P is the vapour pressure at the liquid surface (assumed to be the equilibrium vapour pressure), M is the molecular weight, R is the gas constant and T is the absolute temperature. For pure water at 20°C , P is 17.5 mm Hg (2326 Pa),⁶ M is $0.018 \text{ kg mol}^{-1}$ and J_{max} is therefore $140 \text{ mol s}^{-1} \text{m}^{-2}$. This theoretical maximum rate with α assumed equal to 1 corresponds to a rate of loss of water depth by evaporation of approximately 2.5 mm s^{-1} .

In practice, the evaporation rate of a liquid is much slower (by many orders of magnitude) than the theoretical upper limit described above due to various resistances or barriers to the evaporation process. Commonly, the major resistance arises from the presence of a “stagnant” gaseous layer close to the surface across which the vapour must diffuse. Additional resistance to evaporation caused by the presence of adsorbed monolayers at the liquid surface have been described in the literature.⁷ It is normally assumed that the total resistance to evaporation is obtained by summation of the various resistances. Additional complications may arise at high evaporation rates because evaporation leads to a cooling of the liquid

surface with consequent reduction of the vapour pressure. In this situation, the evaporation rate is coupled to the rate of heat transfer in the surface region. These factors have been considered in detail in the chemical engineering literature.^{8,9}

For pure liquids in the experimental set-up developed here (Fig. 1), we assume that the evaporation resistance arises only from the necessity for vapour diffusion across the gas space (assumed stagnant) between the liquid surface and the exit of the sample tube. Thus, we consider the evaporation flux in the vertical direction J (i.e. evaporation per unit time and area) from a liquid surface of cross-sectional area A across a stagnant vapour space of thickness h , taken to be equal to the distance from the liquid surface to the top of the open sample tube (Fig. 1). Assuming that we need only consider flow in the vertical (x) direction, Fick’s first law gives the instantaneous flux J at any point.

$$J = -D \frac{\partial c}{\partial x} \quad (2)$$

where D is the diffusion coefficient of the vapour through air and c is the concentration of diffusing vapour at position x . The flux J is the flow of vapour per unit area in unit time. Fick’s second law describes the time dependence.

$$\frac{\partial c}{\partial t} = -D \frac{\partial^2 c}{\partial x^2} \quad (3)$$

The observed constant evaporation rate indicates that a steady state is reached relatively rapidly. At steady state, $\partial c/\partial t = 0$ at all points within the stagnant vapour space and thus $\partial c/\partial x = \text{const}$. Therefore, a linear concentration gradient of the evaporating species is established along the vertical axis of the sample tube which we can express as

$$\frac{\partial c}{\partial x} = \frac{c_o - c_s}{h} \quad (4)$$

where c_s is the concentration of vapour just above the liquid surface and c_o is the concentration at the mouth of the open vessel. For a two component gas mixture (diffusing vapour and nitrogen in our case), since there is a concentration gradient of the vapour, there is also a concentration gradient on the second gas component in the opposite direction. Under conditions such that the pressure of the vapour P is much less than the total (atmospheric) pressure P_{atm} , this complication has negligible effect. For $P \ll P_{\text{atm}}$, from eqn. (2) and (4), at the steady state

$$J = -D \frac{c_o - c_s}{h} = V_L c_o \quad (5)$$

The second relationship in eqn. (5) arises because the flux arriving from the liquid surface to the mouth of the sample tube must also equal that carried away by the gas stream with (vertical) mean linear velocity V_L (m s^{-1}). The mean linear flow velocity (V_L) of the gas is related to the volume flow rate (F) according to $V_L = F/A_v$ where A_v is the cross-sectional area of the vessel in the region of the mouth of the sample tube. We note here that it is unclear whether A_v should correspond to the total cross-sectional area of the vessel or the vessel area minus that of the sample tube. Both models are calculated in the comparison with experimental data below where it can be seen that the difference in calculated rates between the two assumptions is small. Solving for c_o yields an equation for J in terms of both h and V_L .

$$J = \left\{ \frac{Dc_s}{h} - \frac{D^2c_s}{h^2V_L + hD} \right\} \quad (6)$$

Noting that $c_s = P/RT$ (assuming the vapour behaves ideally) and that the mass evaporation rate $E = JMA$, we obtain the final equation for E .

$$E = \frac{MADP}{hRT} \left\{ 1 - \frac{D}{hF/A_v + D} \right\} \quad (7)$$

Inspection of eqn. (7) shows that E is predicted to increase with decreasing h (i.e. when the liquid surface gets closer to the sample tube mouth). At low flow rates, E increases with increasing flow rate but becomes independent at high flow rates. As h approaches zero, E is predicted to reach a limiting value given by

$$\lim_{h \rightarrow 0} E = \frac{MAPF}{RTA_v} = \frac{MAPV_L}{RT} \quad (8)$$

For h less than the mean free path of the vapour molecules, we speculate that V_L may be equated with the component of the mean molecular velocity normal to the liquid surface, i.e. $V_L = \sqrt{RT/2\pi M}$. With this substitution, eqn. (8) is then equivalent to the expression for J_{\max} [eqn. (1)] noted earlier.

For diffusing vapours of high vapour pressure so that the condition $P \ll P_{\text{atm}}$ is no longer valid, eqn. (7) must be modified to take account of the effect of the concentration gradient of the second gas component. As described by Jost,¹⁰ this creates an upward convection of the gas mixture. The effect may be accounted for by inclusion of a correction factor z in eqn. (7).

$$E = \frac{MADPz}{hRT} \left\{ 1 - \frac{D}{hF/A_v + D} \right\} \quad (9)$$

where

$$z = \left[\frac{P_{\text{atm}}}{P} \ln \left(\frac{1}{1 - (P/P_{\text{atm}})} \right) \right]$$

In order to test the theoretical predictions of eqn. (9), evaporation rates for pure heptane were measured at 25 °C as functions of both the gas flow rate F and stagnant layer thickness h . Fig. 3 shows the variation of evaporation rate with F for three different values of h . The calculated curves were obtained using eqn. (9) with the parameters noted in the legend. The value of the diffusion coefficient D of heptane in nitrogen at 25 °C used in the calculations ($6.1 \times 10^{-6} \text{ m}^2 \text{ s}^{-1}$) is reasonably close to the literature value ($7.3 \times 10^{-6} \text{ m}^2 \text{ s}^{-1}$).¹¹ The value of the equilibrium vapour pressure was taken from ref. 12. For each set of conditions, two calculated curves are given. The solid line is calculated using A_v equal to

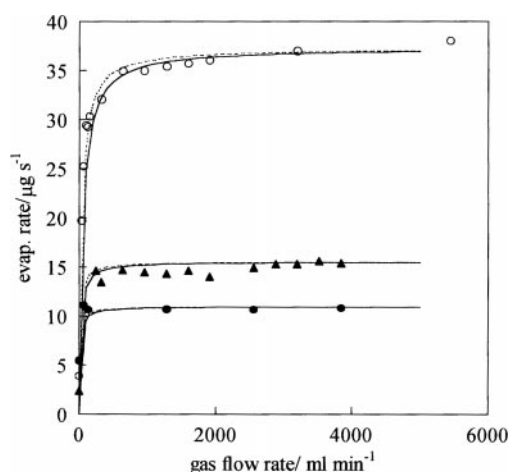


Fig. 3 Variation of heptane evaporation rate at 25 °C with gas flow rate for various fixed values of h . In ascending order, the values of h are 34 (●), 24 (▲) and 10 mm (○). The solid and dashed curves are calculated using eqn. (9) with $M = 100 \text{ g}$, $D = 6.1 \times 10^{-6} \text{ m}^2 \text{ s}^{-1}$, $P = 45.85 \text{ Torr}$ and $A = 2.49 \times 10^{-4} \text{ m}^2$. The solid curves use the total cross sectional area of the vessel ($A_v = 1.26 \times 10^{-3} \text{ m}^2$) whereas the dashed curves refer to the vessel area minus that of the sample tube ($0.91 \times 10^{-3} \text{ m}^2$).

the full cross-sectional area of the vessel. The dashed line uses the full vessel area minus that of the sample tube. The agreement between experiment and theory is reasonably good although the precision does not allow a clear choice to be made concerning the appropriate value of A_v .

According to the assumed model, the physical explanation for the shapes of the plots in Fig. 3 is as follows. At high flow rates (i.e. when the second term in eqn. (9) is negligible and $E \approx MADPz/hRT$), the steady state vapour concentration at the mouth of the sample tube (c_0) approaches zero and the evaporation rate reaches a flow rate independent plateau value. The magnitude of the plateau value scales as $1/h$. At lower flow rates, c_0 increases giving a lower concentration gradient and reduced evaporation rate. At zero flow rate, eqn. (9) predicts zero evaporation rate for macroscopic values of h . In practice, the intercepts of the curves in Fig. 3 (shown also in Fig. 4) are small but finite and are presumably due to vapour diffusion within the stagnant vapour space of the entire volume of the vessel. We note here that the zero imposed flow rate values are sensitive to the extent to which the mouth of the measurement vessel is shielded from extraneous draughts.

The variation of evaporation rate with h at various fixed gas flow rates is shown in Fig. 4. The solid and dashed calculated lines, calculated using the same input parameters, again show reasonable agreement with experiment, even for h values as low as a few mm. To obtain reproducible data at the low h values, care had to be taken to ensure that the heptane did not wet up the walls of the sample tube during loading. Such wetting, giving an increased liquid surface area and a lower mean value of h , was found to give an initial evaporation rate higher than expected. Overall, it can be concluded that accurate rate data which is well described by the assumed model can be obtained for h greater than approximately 10 mm and flow rates of 500 to 4000 ml min⁻¹.

The volumetric gas flow rate within the vessel was varied from 0 to approximately 5000 ml min⁻¹. This corresponds to a range of mean linear gas velocities of 0 to 0.09 m s⁻¹. Thus, the maximum Reynolds number (equal to $\rho_g V_L d/\eta$ where ρ_g is the gas density, d is the vessel diameter and η is the gas viscosity) is approximately 200. Because of the complex geometry of the gas flow around the sample tube, it is unclear whether the gas flow is laminar or turbulent.⁹

It is interesting to compare evaporation rates under our experimental conditions (i.e. a liquid in a partially filled tube exposed to vertical gas flow) with the data of Prata and

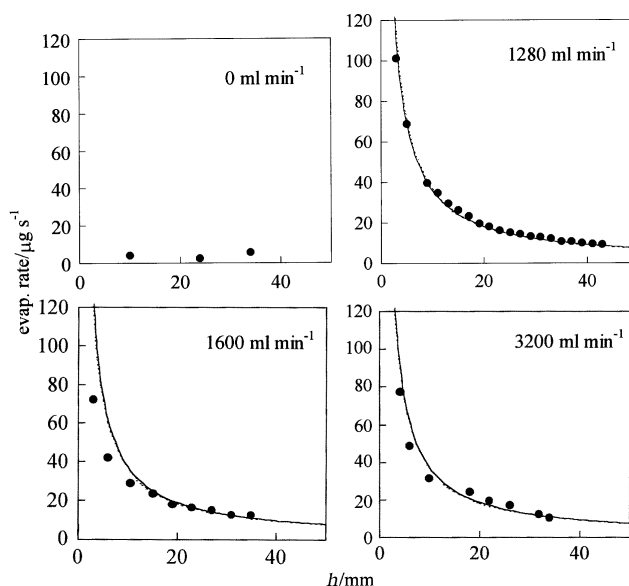


Fig. 4 Variation of heptane evaporation rate at 25 °C with h for fixed gas flow rates (marked on the plots). The solid and dashed lines are calculated using the same parameters as in Fig. 3.

Sparrow.¹³ They determined evaporation rates of cumene and toluene from a partially filled container in a horizontal, turbulent gas flow over the container mouth. Their measured rates are approximately an order of magnitude higher than those calculated using eqn. (7). The origin of this effect is probably that the horizontal gas flow is likely to be deflected into the sample container at the downstream lip of the container. This would disrupt the steady state vapour concentration gradient found under the conditions used in our study. As observed by Prata and Sparrow, the evaporation rate under their conditions shows a complex dependence on gas flow rate and h which is not amenable to quantitative analysis.

In addition to measuring the initial evaporation rates (where the change in h over the experimental run can be neglected), we have also recorded mass loss curves for volatile liquids where h does increase during the run. Under conditions of high gas flow rates when $E \approx MADP_z/hRT$, substitution of $E = -dm/dt$ and $h = (h_t - m/\rho A)$ where m is the mass of liquid sample remaining, h_t is the total inner height of the sample tube and ρ is the liquid density, followed by integration yields the following relationship between m and t .

$$t = \frac{RT h_t}{MADP_z} (m_0 - m) - \frac{RT}{2\rho MA^2 DP} (m_0^2 - m^2) \quad (10)$$

where m_0 is the initial mass of liquid at time zero.

In Fig. 5 we compare measured mass loss versus time curves for pentane and hexane with those calculated using eqn. (10) with the parameters listed in the figure legend. In the experimental curves, the evaporation rate decreases with increasing time as h increases. The curve for hexane is well described by eqn. (10) and the value of D obtained from the best fit curve is in agreement with the range of literature values shown in Table 1. Significant deviations between theory and experiment are seen for the more volatile pentane. In particular, the initial (fastest) evaporation rate for pentane is slower than the calcu-

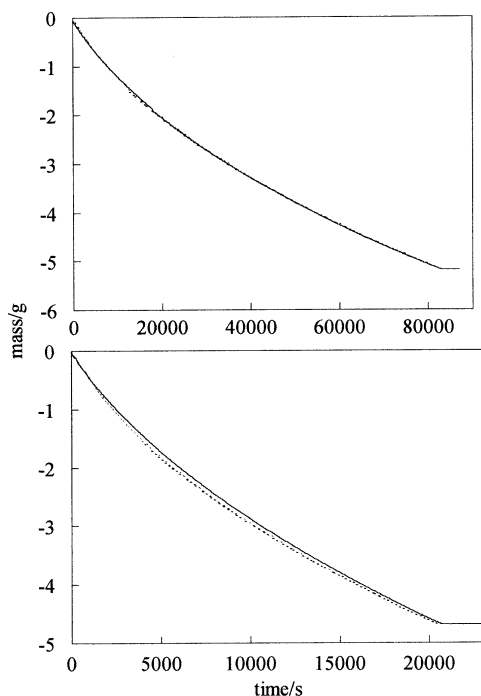


Fig. 5 Plots of sample mass versus time for the evaporation of hexane (upper plot) and pentane (lower plot) at 25.0 °C. The solid lines (actually closely spaced data points) are the experimental data and the dashed lines are calculated using eqn. (9) with $h_t = 40$ mm and other apparatus constants as in Fig. 3. For hexane, $D = 7.90 \times 10^{-6} \text{ m}^2 \text{ s}^{-1}$, $P = 151.5$ Torr, $\rho = 654.7 \text{ kg m}^{-3}$ and $m_0 = 5.116$ g. For pentane, $D = 6.85 \times 10^{-6} \text{ m}^2 \text{ s}^{-1}$, $P = 512.8$ Torr, $\rho = 621.2 \text{ kg m}^{-3}$ and $m_0 = 4.689$ g. D values were adjusted to obtain the best fits to the experimental data.

Table 1 Literature values of vapour pressure P and vapour diffusion coefficient D in either nitrogen or air for pure liquids at 25 °C

Liquid	P/Torr	$D^b/10^{-6} \text{ m}^2 \text{ s}^{-1}$
water	23.76(6)	24.0(14) ^c
n-pentane	512.8(12)	8.42(15)
n-hexane	151.5(12)	8.2(14), ^c 7.32(15), 8.1(17) ^c
n-heptane	45.85(12)	7.3(11) ^c
n-octane	14.14(12)	6.16(15), 6.02(16), 6.9(17) ^c
n-decane	1.35(12)	5.7(17) ^c
n-dodecane	0.135(12)	5.0 ^d
benzene	95.18(12)	9.32(15), 9.37(18) ^c
cyclohexane	97.61(12)	7.8(14), ^c 8.1(17), ^c 7.95(18) ^c
ethanol	57.13(6)	11.8(15), 13.1(14) ^c

^a Numbers in parentheses refer to the literature references. ^b Where multiple values of D are given, the mean value was used in Fig. 6. ^c Corrected to 25 °C using the equation quoted in ref. 15. ^d Estimated by extrapolation from data for the linear chain alkanes.

lated value and the “best fit” value of D is anomalously low. A likely explanation for this effect is that the very high evaporation rate in this case leads to significant cooling of the pentane surface causing the evaporation rate to be lower than predicted. Under these conditions, the evaporation rate is expected to be coupled to the heat conduction rate. Consistent with this explanation, the deviations are absent for hexane where the evaporation rate is slower.

We now consider the mass evaporation rates for a range of different pure liquids. Under conditions of high gas flow rates when $E \approx MADP_z/hRT$, the factor MDP_z/RT is a measure of the mass “evaporability” for a liquid of unit surface area at unit value of h . Using literature values of D and P listed in Table 1, we compare calculated values of MDP_z/RT and values of Eh/A derived from evaporation rate measurements under high gas flow rate conditions for a range of pure liquids (Fig. 6). It can be seen that the agreement between measured and predicted evaporation rates is reasonably good for liquids for which the evaporation rates span over 3 orders of magnitude. We note that the magnitude of the discrepancies between the measured and calculated values (10 to 20%) is of the same order as the variation of the literature values of D seen in Table 1.

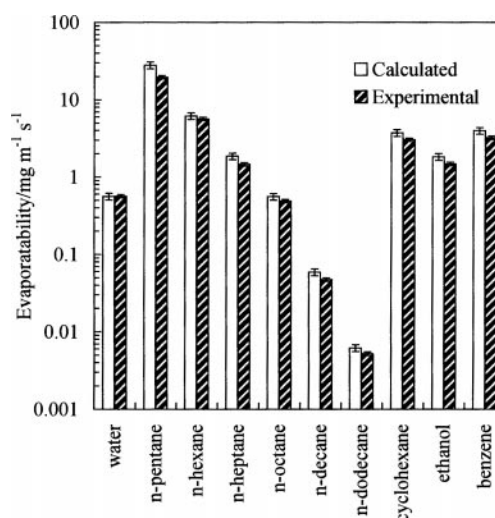


Fig. 6 Comparison of calculated and measured evaporability values for a range of pure liquids at 25 °C. Calculated values (= MDP_z/RT) were obtained using the literature values listed in Table 1. Measured values refer to Eh/A derived from initial evaporation rates.

Conclusions

We have shown that the experimental arrangement described here can be used to determine absolute liquid evaporation rates with an accuracy of a few percent. The simple model successfully accounts for the variation of measured rate with gas flow rate and stagnant vapour space thickness h . Evaporation rates for liquids with vapour pressures ranging from 500 to 0.1 Torr have been measured and show reasonable agreement with predicted values. The utility of the method lies in the fact that it yields absolute evaporation rates without complications due to complex gas flow patterns. We are currently extending the use of the technique to examine the evaporation rates from complex systems such as emulsions, liquids contained within porous solids and other colloidal formulations.

Acknowledgements

We thank Dr M. T. McKechnie of Reckitt & Colman Products for helpful discussions. We are grateful to Reckitt & Colman Products and the University of Hull for funding. We thank Mr Ilian Todorov for the measurements of n -dodecane.

References

- 1 I. Langmuir and V. Schaefer, *J. Franklin Institute*, 1943, **235**, 119.
- 2 R. J. Archer and V. K. La Mer, *J. Phys. Chem.*, 1955, **59**, 200.
- 3 T. B. Hine, *Physical Rev.*, 1924, **24**, 79.

- 4 S. H. Wade, *Trans. Inst. Chem. Eng.*, 1942, **20**, 1. [View Article Online](#)
- 5 See, for example, N. K. Adam, *The Physics and Chemistry of Surfaces*, Oxford Clarendon Press, 2nd edn., 1938.
- 6 *CRC Handbook of Chemistry and Physics*, CRC Press Inc., Boca Raton, 62nd edn., 1981.
- 7 See, for example, *Retardation of Evaporation by Monolayers: Transport Processes*, ed. V. K. De La Mer, Academic Press, New York, 1962.
- 8 See, for example, T. K. Sherwood, R. L. Pigford and C. R. Wilke, *Mass Transfer*, Chem. Eng. Series, McGraw-Hill, New York, 1975.
- 9 See, for example, J. R. Welty, C. E. Wicks and R. E. Wilson, *Fundamentals of Momentum, Heat and Mass Transfer*, 3rd edn., John Wiley & Sons Inc., New York, 1984.
- 10 W. Jost, *Diffusion in Solids, Liquids and Gases*, Academic Press Inc., New York, 1952, p. 9.
- 11 L. T. Carmichael, B. H. Sage and W. N. Lacey, *Am. Inst. Chem. Eng. J.*, 1955, **1**, 385.
- 12 *Selected Values of Properties of Hydrocarbons and related Compounds*, Thermodynamics Research Center, AP144, Texas A&M University, 1978.
- 13 A. T. Prata and E. M. Sparrow, *Can. J. Chem. Eng.*, 1986, **64**, 511.
- 14 R. C. Reid, J. N. Prausnitz and T. K. Sherwood, *The Properties of Liquids and Gases*, 3rd edn., McGraw-Hill, New York, 1977.
- 15 G. A. Lugg, *Anal. Chem.*, 1968, **40**, 1072.
- 16 E. Mack, Jr., *J. Am. Chem. Soc.*, 1925, **47**, 2468.
- 17 G. A. McD. Cummings and A. R. Ubbelohde, *J. Chem. Soc.*, 1953, 3751.
- 18 G. H. Hudson, J. C. McCoubrey and A. R. Ubbelohde, *Trans. Faraday Soc.*, 1960, **56**, 1144.

Paper 8/05344H